applied sciences

MDPI

*Article*

# Advanced Coatings of Polyureas for Building Blast Protection: Physical, Chemical, Thermal and Mechanical Characterization

**Fernando Leite [1,2,*], Carlos Mota [1,2], João Bessa [1,2], Fernando Cunha [1,2], Raul Fangueiro [1,2,3], Gabriel Gomes [4] and José Mingote [5]**

[1] Centre for Textile Science and Technology, School of Engineering, University of Minho—Campus of Azurém, 4800-058 Guimarães, Portugal
[2] Fibrenamics Association—Institute for Innovation in Fibrous and Composite Materials, University of Minho—Campus of Azurém, 4800-058 Guimarães, Portugal
[3] Department of Mechanical Engineering, University of Minho—Campus of Azurém, 4800-058 Guimarães, Portugal
[4] Military Academy Research Center (CINAMIL), Instituto Universitário Militar, Rua Gomes Freire, 1169-203 Lisbon, Portugal
[5] NATO Counter Improvised Explosive Devices Centre of Excellence (C-IED COE), Hoyo de Manzanares, 28240 Madrid, Spain
* Correspondence: fernandoleite@fibrenamics.com

**Abstract:** Due to the increase in the global terrorist threat, there has been a growing demand for materials that can more efficiently protect civil, industrial, and military structures against explosions. In this sense, two new commercial polyureas (A and B), that present high potential to be used as a protective coating on building facades against explosions, were compared in this work, through several tests. Chemical characterization with the Scanning Electron Microscope (SEM) of the surface of the polyureas revealed that the commercial polyurea A has a heterogeneous surface while the other polyurea has a more uniform and homogeneous surface, resulting in a more compact structure. The shock-wave attenuation ability of polyurea is believed to be controlled primarily by the hard domains. The TGA tests revealed that polyurea B has more hard segments than polyurea A in its composition. The mechanical tests performed showed that polyurea B has significantly better tensile properties-almost 3000% of maximum deformation capacity compared with approximately 115% of polyurea A. Thus, it was concluded that polyurea B has more potential to be used as a coating in building blast protection due to its exceptional elongation characteristics, a critical parameter to absorb the high frequency and intensity of blasts.

**Keywords:** polyurea; blast protection; elongation; coating



**Citation:** Leite, F.; Mota, C.; Bessa, J.; Cunha, F.; Fangueiro, R.; Gomes, G.; Mingote, J. Advanced Coatings of Polyureas for Building Blast Protection: Physical, Chemical, Thermal and Mechanical Characterization. *Appl. Sci.* **2022**, *12*, 10879. https://doi.org/10.3390/app122110879

Academic Editors: Theodore E. Matikas and Jacek Tomków

Received: 16 September 2022
Accepted: 24 October 2022
Published: 27 October 2022



## 1. Introduction

The ever-increasing safety requirements demanded in the engineering and construction of structures to protect people from terrorist threats or industrial accidents are fostering the study and development of new materials and processes. Polyurea are one of these versatile engineering materials, which has been commercially available since the early 1990s. They have the processing conditions and performance properties which allow the application of this type of material as a coating in a wide range of industries, like defense, security, construction, and automotive [1–3]. According to the Polyurea Development Association (PDA), polyureas result from the combination of two components: isocyanate and synthetic resin blend, such as amine-terminated polymer resins and (or) amine-terminated chain extenders.

The isocyanate component of the polyurea can be aromatic or aliphatic in nature. It can be a monomer, a polymer, or a variant reaction of isocyanates, a quasi-prepolymer, or a prepolymer. The prepolymer, or a quasi-prepolymer, can be made of an amine-terminated polymer resin or a hydroxyl-terminated polymer resin. The resin blend is an

amine-terminated polymer resin and (or) amine-terminated chain extenders [4]. Polyureas have great abrasion resistant capacity, that combined with its exceptional physical properties, such as high hardness, flexibility, tear strength, tensile strength, and chemical and water resistance, that makes this material ideal as a coating in applications that have very demanding functional requirements. The reaction that forms the polyurea is rapid with gel times measured in seconds, which means the reaction proceeds largely independently of ambient temperature and humidity, facilitating application of polyurea under diverse conditions. An important concern associated with polyurea coatings is the requirement of rapid mixing of the reactants, an issue which has been overcome using a suitable mixing module by impingement at high pressures. The viscosity of both components (isocyanate and resin) needs to be almost equal (difference less than 100 mPa·s), which mandates a heating arrangement, with higher viscosity reactants requiring higher pressures for spraying. It is to be noted that the spraying pressure and reaction temperature of the reactants greatly affects the properties of the product formed. The micro-structure polyureas are comprised of two distinct domains, the hard domains, formed by hydrogen bonded polar urea linkages (–NH–CO–NH–), and the soft domains that consist of well-mixed hard and soft long chain aliphatic chains. Discrete hard domains are formed only when the molecular weight of the soft segment cross a particular threshold [5]. Polyureas are ideal coatings in new engineering projects of the infrastructure industry or the refurbished and maintenance of the existing ones. The high durability and strong resistance polyureas make them a very interesting choice for situations where the impact energy of earthquakes or blast phenomena must be dissipated [4]. The worldwide increase in terrorist activity and its lethality has exposed the weaknesses of the existing infrastructure to blast loading, particularly when large amounts of explosives are used (Figure 1). According to data collected from 1970–2017 by the National Consortium for the study of Terrorism and Response to Terrorism, bombings and (or) explosions compromise approximately 49% (88,600 incidents) of the total numbers of terrorist attacks (182,300 incidents) [6]. Thus, significant research projects have been developed within the last years to retrofit building and vehicle structures to resist blast loading. Retrofitting systems are inexpensive, easy to install, and protect the occupants of the facilities [7].

**Figure 1.** Structure damaged by a Vehicle-Borne Improvised Explosive Device (VBIED) explosion (Burgos, 2009).

In the case of buildings typically, the main structure withstands the blast, but the facades are destroyed as well as non-structural masonry partitions, elevator and stairway shafts, furniture, drop ceilings, and light fixtures, which are propelled at high velocities hitting the occupants. A blasting explosion, associated with terrorist threats, is a dynamic load characterized by its short duration with high intensity and frequency load. The design of most structures did not predict the need for the buildings to withstand the

high dynamic loads caused by the detonation of bombs. It is generally accepted that the structural disintegration and propulsion of the debris results in more casualties than the ones resulting from the explosion itself. The retrofitting of existing structures to enhance their strength diminishes the extent of the damage generated from explosions. One of the retrofitting solutions, which has emerged as an economically viable solution, is the application of polyurea coatings. The most important characteristics of any retrofitting polyurea include ease of application, rapid cure time, adhesive properties, and excellent mechanical properties, particularly strength and elongation. The polyureas subjected to blast and impact loads tend to exhibit high strain to failure, thereby absorbing, dissipating, and mitigating the energy arising from dynamic loads. The mechanical properties of the polyurea are the main factor to contain and absorb the high intensity and velocity fragments generated from the blast.

Conventional retrofitting of facades or non-structural elements in general (masonry and glazing) usually focus on adding mass to the system, increasing the thickness by adding internal masonry, concrete, or metal walls [8]. Addition of internal metallic frames are also widespread, seeking to reduce the free span of the walls. Construction techniques that try to increase the strength of structures against explosions through the incorporation of steel or concrete are hard to implement, time consuming, expensive [9], and could increase the debris hazard. In turn, retrofit techniques that focus on ductility, instead of increasing the mass of the structural element, may be more beneficial.

From the few direct comparisons between the performance of structures retrofitted with different types of composites, with equal thickness, ref. [10] the conclusion is that the hybrid composite aramid/glass performed better than the Carbon Fiber Reinforced Polymer (CFRP) composite because the flexibility of the hybrid increased.

Effectively, the use of elastomers-particularly polyurea applied to the surface of walls [11] can present an appealing alternative in minimizing the damage caused by the blast to the underlying structure and personnel. The use of polymers seems to offer good benefits for the retrofitting of masonry, providing an increase in ductility, allowing significant deflections outside the plane of the wall.

The main difference between blast loads and other dynamic loadings is the impulsive nature from the first ones, where the duration is usually very brief and generates high pressures [12]. The key to overcoming these threats is to ensure the external wall of the building can survive the bomb blast without breaking apart and simultaneously not load unacceptably the supporting columns.

The shock-wave attenuation ability of polyurea is believed to be controlled primarily by the hard domains. Presently, there is no general consensus regarding the mechanism underlying polyurea-induced shock-wave mitigation. The most accepted mechanisms include the following:

- Shock-wave-induced hard-domain compaction and ordering, where the extent of this blast-mitigation effect is expected to be directly proportional to the hard-domain volume fraction;
- Shock-wave-induced hard domain crystallization/densification, where the hard domains of the polyurea experience irreversible compaction and densification with an associated increase in their degree of order upon being subjected to shock-wave loading;
- Shock wave induced hydrogen bond cleavage and formation, where the exposure to shock loadings leads to the cleavage of bi-dentate H-bond between the urea linkages, which subsequently rearrange to form more numerous H-bonds within the hard domains, thereby leading to the absorption and dispersion of shock energy;
- Shockwave-capture-and-neutralization, shock waves travel as a single wave in homogeneous materials. However, upon loading of a layered heterogeneous material system, e.g., polyurea, a two-wave structure is obtained: a leading shock front followed by a complex pattern that varies with time. This dual shock-wave pattern is attributed to the material architecture through which shock wave propagates, i.e., the impedance (and geometric) mismatch present at various length scales, and nonlinearities arising

from material inelasticity and failure. This secondary trailing shock-wave (release wave), reportedly catches up with and attenuates the leading shockwave, thereby leading to shock attenuation [13].

In work presented by Wang et al. [14], a polyurea layer reinforced clay brick masonry resulted in a considerable improvement of the blast resistance of the structure. An adjustment in the proportion between the isocyanate and amino groups of the polyurea led to increased NCO content in the prepolymer. The tensile strength at break and the breaking elongation ratio obtained were 23 MPa and 510%, respectively. Consequently, the energy absorption capability in the polyurea increased, reinforcing the structure.

Iqbal et al. [15] reported an optimal ratio of chain extender to optimize the H-bonding, which improves the mechanical properties. In the work of Iqbal et al., a commercial isocyanate prepolymer, Suprasec®2054, NCO = 15.5% was used with Poly (propylene oxide) (PPO) with the commercial name JEFFAMINE®D-230 and JEFFAMINE®D-200. The presence of a chain extender, diethyl-toluene diamine, increased the vicinity of urea linkages, which in turn favored the formation of H-bonds in the hard segment. The mitigation of the explosion increased with the coating thickness. A polyurea coating with six mm thickness could withstand fragmentation pressures higher than 90 psi [15].

Raman et. al. [12] studied the positive effects of using polymers for retrofitting reinforced concrete structures subjected to blast loads by conducting a numerical investigation on the behavior of an unretrofitted reinforced concrete panel subjected to the blast load from a 2 kg charge at 1.6 m stand-off distance, and subsequently comparing its performance with several polymer coated panels. The increment of the thickness of the polyurea coating did not significantly influence the reduction of the displacement. The application of the polyurea coating on the non-blast-facing side of the panel tends to increase the effectiveness of displacement control.

Miao et al. [3] studied the mechanical behavior and equivalent configuration of a polyurea under wide strain rate range. The polyurea with the commercial name of Paxcon®PX-3350, developed by LINE-X LLC, had a three mm thickness. The isocyanate and resin components of the polyurea were preheated at 60 °C, then mixed under high pressure (2000–2500 psi) with specific pressure equipment before applying the polyurea by spray coating. The polyurea's stress-strain curves shared a similar mechanical and strain hardening coefficient trend under different strain rate loads (between 0.001–2800 $s^{-1}$).

J. S. Davidson et al. [16], carried out three ballistic tests with samples in the shape of brick walls fixed in steel frames. In samples one and two, the wall panels were coated with polyurea only in the inside face, while the third panel took a coating on both sides. The performance tests showed that applying the polyurea coating only on one side of the wall can effectively increase its resistance against shock waves.

Guo et al. [17] studied polyureas formed by the reaction of isocyanate Isonate 143 L from Dow Chemical and amine-terminated resin blend Versalink®P-650 or Versalink®P-1000 from Air Products. The chemical composition of the polyurea samples was altered to provide different hard segment ratios. The sample PU605, made with Versalink P-650 with 105% molar equivalent Isonate 143 L, is stiffer than the sample PU105, developed by mixing Versalink P-1000 with 105% molar equivalent Isonate 143 L.

Baylot et al. [18] studied the blast response of lightly attached concrete masonry unit walls with several different types of retrofits:

1. A one mm thick Fiber Reinforced Polymer (FRP) with a modulus of elasticity of 26.13 MPa, a tensile strength of 600 MPa, a 2.24% elongation at break, and a density of 0.915 $kg/m^2$.
2. A polyurea with an elastic modulus of 234 MPa, secant modulus of 165 MPa, yield strength of 11.5 MPa, and tensile strength of 13.8 MPa. The elongation at yield and rupture are 4.7 and 89%, respectively.
3. A one mm thick sheet hot-dipped in A-36 galvanized steel placed behind the wall.

The three retrofit types were tested at the same loading level, which caused the non-retrofitted wall to fail at a velocity of 8.2 m/s. The results show that the FRP and polyurea

retrofits prevented the debris from entering the structure, therefore, were considered successful retrofits.

In this study, two commercial polyurea were compared to determine their capability to be used as a coating for explosion protection on building facades. An extensive plan of tests was designed and performed to evaluate this possibility. The procedure of tests included physical, chemical, thermal, and mechanical characterization of the polyureas samples.

## 2. Materials and Methods

### *2.1. Raw Materials*

The polyureas analyzed in this study are fast-set hybrid polyureas that are 100% solids and Volatile Organic Compound (VOC) free. The polyureas used in the R&D Project "Protection of Infrastructures and Systems Against Explosives–Advanced Protective Coatings (PRINSE-APC)" project managed and led by the NATO Counter Improvised Explosive Devices Centre of Excellence (C-IED COE). The main goal of the PRINSE project was to characterize the properties of existing high quality commercially available elastomers to obtain an enhanced protective system against blast threats and fragments using theoretical and experimental research.

### *2.2. Production of Samples*

Before producing the polyurea, the components A -isocyanate- and B-resin mix-of both polyureas were pre-conditioned at a temperature of 30 °C. The polyureas were applied at 70 °C with a pressure of 6 bar, in a 1:1 ratio by volume between the two components. The polyureas were applied using spray equipment, which generated adequate fluid pressure for proper mixing and best polymerization results. This technique, known as a hot spray, is the most used because of its quick cure time and great productivity compared to the traditional application methods.

### *2.3. Characterization*

The chemical analysis tests determined the chemical bonds and elemental composition of the polyureas, while the thermal characterization of the polyureas determined the degradation temperature of the materials. The physical tests characterized the density, water absorption, and dimensional stability of the polyureas. Finally, the mechanical tests assessed the Shore D hardness, the tensile, and the compression properties of the materials studied.

#### 2.3.1. Chemical Analysis

The Fourier Transform Infrared Spectroscopy (FTIR) tests performed on the polyureas were carried out according to the standard ASTM E1252, performing 60 scans with a resolution of 16 $cm^{-1}$ to obtain an IR spectrum in the range of 4000–550 $cm^{-1}$.

#### 2.3.2. Thermal Characterization

The degradation and mass loss of the polyureas were determined using the Differential Scanning Calorimetry (DSC) and Thermogravimetric Analysis (TGA) techniques. In the DSC tests, performed according to the standard ASTM D 3418, the heating rate used was 10 °C/min, until 500 °C was reached. In the TGA tests, carried out according to the standard ISO 11358, the sample was subjected to an inert environment with $N_2$ gas to provide the adequate test ambient. The gas environment was suitable for thermal decomposition, and the heating speed used was 10 °C/min until a maximum temperature of 910 °C.

#### 2.3.3. Physical Analysis

The Scanning Electron Microscope (SEM) tests were used to evaluate the morphological structure of the samples were performed in an Ultra-high-resolution Field Emission Scanning Electron Microscopy (FESEM). Before the analysis, the polyureas were covered with a thin film of Au-Pd (80–20 wt.%), using a high-resolution sputter coater. Secondary

electron images, i.e., topographic images, were obtained at an acceleration voltage of 10 keV. Atomic contrast images were obtained using a Backscattering Electron Detector (BSED) at an acceleration voltage of 15 keV. After these tests, the samples were analyzed between 0 and 10 keV in the Energy Dispersive X-ray (EDX) to determine the elementary composition of the polyureas.

The density of the polyureas was determined following the standard ISO 1183, using the immersion method which determines the density of solid substances. It was possible to determine the density of the samples using specimens with 10 × 10 mm, using an analytical balance and distilled water as the immersion liquid.

For the water absorption test, the samples had dimensions of 10 × 10 × 2 mm, which were first placed in an oven for 24 h at 50 °C, following the standard ASTM D570. Subsequently, after weighing, the samples were immersed in distilled water for 24 h and weighed again after that period had passed. The percentage of water absorption was determined using Equation (1):

$$\% \text{ Water absorption} = (mf - mi)/mi \times 100 \quad (1)$$

where mf and mi represent the final and initial mass of the samples tested, respectively.

In the dimensional stability test, performed according to the standard ASTM D1204, the dimensions of a specimen of the polyureas were registered using reference marks. The sample was then placed in an oven for 24 h, at 70 °C. After that period, the samples were exposed to room temperature for one hour then a new measurement was made.

#### 2.3.4. Mechanical Characterization

The tensile tests were conducted on a universal testing machine, according to the ASTM D412 standard, in which five specimens of the polyureas sample were tested with a crosshead speed of 15 mm/min and a gauge length of 10 mm. A 100 kN load cell was used to stretch the specimens until failure-yield or fracture. The tensile strength, $T_{(xxx)}$), at a specific (xxx)% elongation, and the elongation (E), at any degree of an extension, were calculated by Equations (2) and (3) respectively:

$$T_{(xxx)} = F_{(xxx)}/A \quad (2)$$

$$E = 100\ ((L - L_o))/L_o \quad (3)$$

where $F_{(xxx)}$ is the force at a specified elongation, A is the cross-sectional area of the unstrained specimen, L is the observed distance between benchmarks on the extended specimen and $L_o$ is the original distance between benchmarks.

The compression tests were carried out according to the standard ISO 604 to determine the modulus and compressive strength of the polyureas. The speed used to determine the compression modulus and the compressive strength was 1 mm/min and 5 mm/min, respectively. Type A specimens were used to determine the modulus of elasticity and Type B to determine the compressive strength, both with a resistant cross-section of 10 × 7 mm.

The test method used to measure Shore D hardness of the polyureas was following the standard ASTM D2240. During the hardness tests, the durometer indenter foot penetrated the samples for 3 or 15 s.

## 3. Results

### *3.1. Chemical Analysis of the Polyurea*

The results of the FTIR test for both polyurea presented in Figure 2 show the bonds that constitute the two separate microphases segments of the polyurea. The two polyureas have very similar FTIR spectrums since no significant differences exist between the chemical structure of both polyureas.

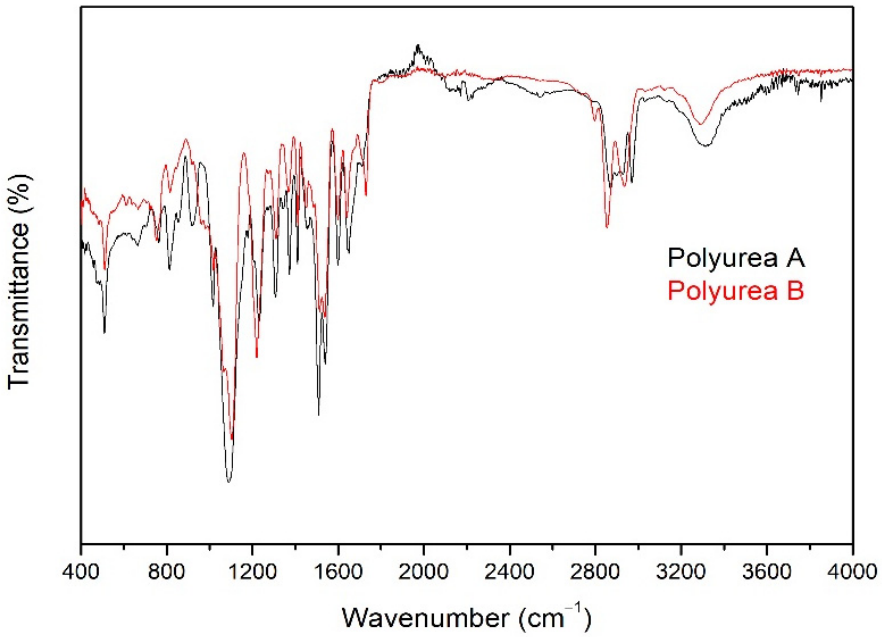


**Figure 2.** Comparison of FTIR spectra of polyureas A and B.

The soft segment of the polyureas consists of long aliphatic polyether chains and forms amorphous domains, while the hard portion is composed urea bonds [19–22].

The hard segment domains of both polyureas present at 3284–3287 cm$^{-1}$ correspond to N–H stretching vibrations. The band between 1600–1700 cm$^{-1}$ represents C=O stretching vibrations, is only present in polyurea B. The blast mitigation ability of the polyurea is controlled primarily by their hard domains. The irreversible densification and order-which increases upon the application of shock wave loads-of the hard realms of the polyurea lead to the shock wave attenuation and dispersion mechanisms that characterize this type of material. The extent of this blast mitigation effect is proportional to the hard domain volume fraction contained in the polyurea [13].

The absorption bands that correspond to the C–N stretching vibrations are present at around 1540 cm$^{-1}$ [23]. The strong absorption peak at approximately 1080 cm$^{-1}$ corresponds to the isocyanate CN stretch alkyl amine group attached. The FTIR spectrum also shows the stretching vibrations for CH stretch alkane at proximately 2970 cm$^{-1}$, respectively.

Finally, the contributing structures CO stretch carboxylic, alcohol, and anhydride are represented in the absorption peak at 1300 cm$^{-1}$, 1230 cm$^{-1}$, and 925 cm$^{-1}$, respectively [24].

### *3.2. Thermal Analysis Results*

The DSC graphic of polyureas A and B is shown in Figure 3. In this graphic, it is possible to observe that polyurea A has two peaks which correspond to two degradation stages. The first peak, around 330 °C, is attributed to the degradation of the hard segment part of the polyurea due to the relatively low thermal stability of the urea group. Previously, studies using hyphenated techniques have revealed that this initial decomposition step leads to evolution of carbon dioxide primarily. The subsequent mass loss, around 410 °C, occurs due to the pyrolytic decomposition of the soft segments, polyether linkages in the present case, leading to evolution of hydrocarbons in larger amounts [25]. The mass loss associated with the first and second stages vary with the percentage of hard segment present in the composition. The DSC curve of polyurea B is similar to the DSC curve of polyurea A. However, the first degradation stage starts closer to 300 °C, while the second degradation stage of this polyurea is not so distinguishable as was in the case of polyurea A.

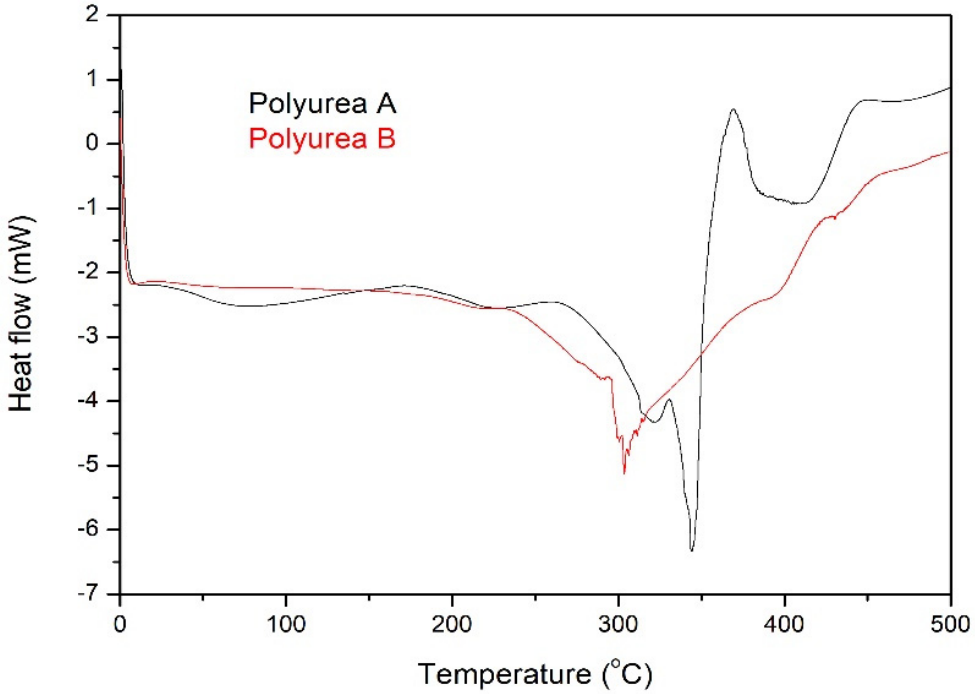


**Figure 3.** DSC plot of polyureas A and B.

The TGA analysis performed on polyurea A is shown in Figure 4. In analyzing the TGA graphic presented, it is possible to observe that the DTG curve that corresponds to the derivative loss of mass for polyurea A (blue line) has two peaks, representing the two degradation stages defined in the DSC graphic of Figure 3. These two degradation stages of polyurea A correspond to a total mass loss of 93.1%, represented by the black line.

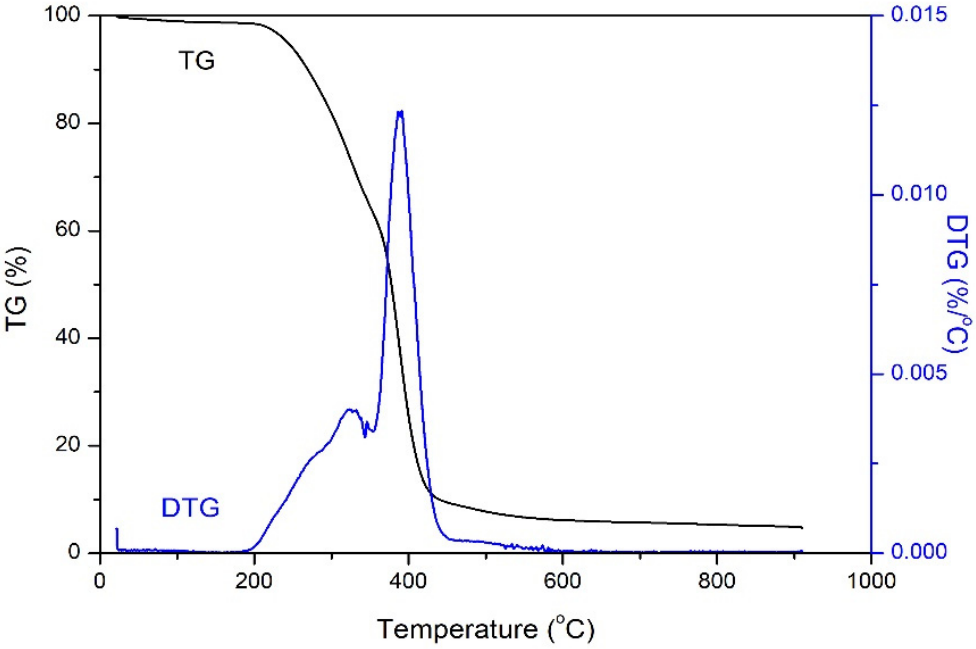


**Figure 4.** TGA analysis of polyurea A.

The blue line in Figure 5 represents the DTG curve of polyurea B. In this curve the presence of two stages of polyurea degradation is clearer, contrary to what was seen in the DSC curve of this material. The first degradation stage starts at around 300 °C, while the second one is near 400 °C. The polyurea B tested sample presented a mass loss of 96.3%,

represented in the graphic of the Figure 5 by the black line. From the TG curves, presented in Figures 4 and 5, it is possible to observe that the first step is shorter than the second degradation stage, on the case of polyurea A, meaning that this polyurea has less hard segments in its composition. The reverse happened in the case of polyurea B, that has a longer first step of degradation, thus has more hard segments in its compositions than soft segments. Like it was referred beforehand, the hard segments are responsible for the shock-wave attenuation ability of polyurea.

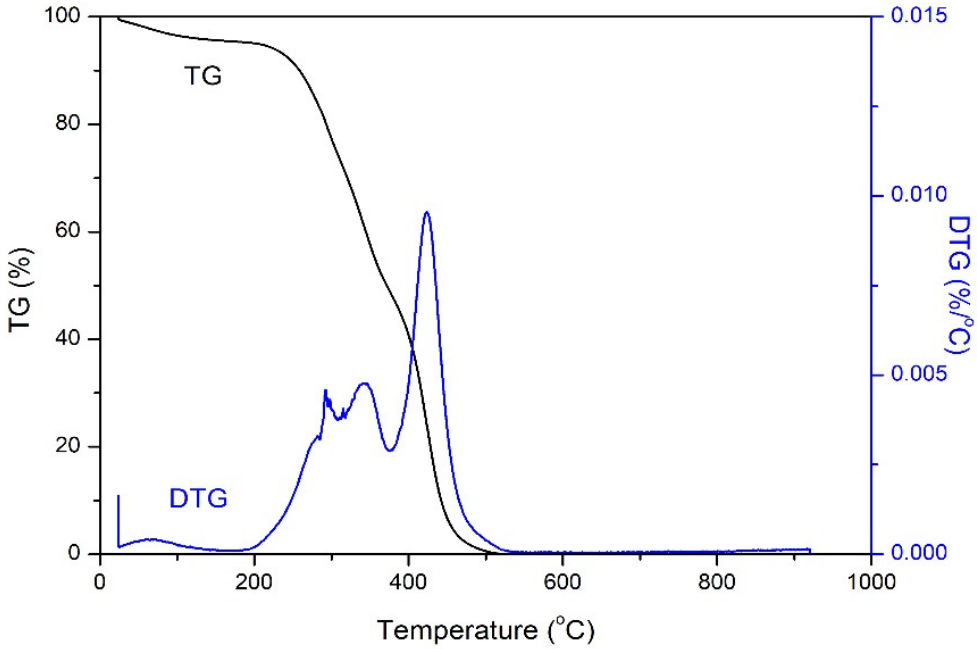


**Figure 5.** TGA analysis of polyurea B.

### *3.3. Physical Characterization Results*

The images taken with SEM for both polyureas are presented in Figure 6. The images show that polyurea A has a heterogeneous surface, while polyurea B has a more homogeneous surface. Some zones of both polyureas were highlighted and then analyzed separately, using the EDX technique to identify the chemical elements present in the materials used in this study.

The results obtained from the EDX technique, presented in Figure 7, show that the main chemical elements of both polyureas are carbon and oxygen. Nitrogen was identified in some areas of both polyureas, while aluminium, silicon, and titanium were present in only one of the polyureas. Aluminium and silicon were observed only in polyurea A and titanium appeared only in polyurea B. Some other chemical elements are present. However, their presence is residual. It is worth mentioning the appearance of titanium in polyurea B since titanium nanoparticles are commonly used in composites to improve the mechanical properties of materials.

The physical properties of the polyureas were evaluated through density, water absorption, and dimensional stability tests. The density of both polyureas, presented in Table 1, are similar.

Both polyureas had slight variations in mass, 0.94% $\pm$ 0.04% for polyurea A and 1.12% $\pm$ 0.04% for polyurea B, after being immersed for 24 h in distilled water, meaning the amount of water absorbed by both polyureas was minimum. These values are consistent with the intrinsic characteristics of these types of materials since they are water resistant. Thus, polyureas are being used as coatings in several industries where the products are or could be in direct contact with water [23,26,27].

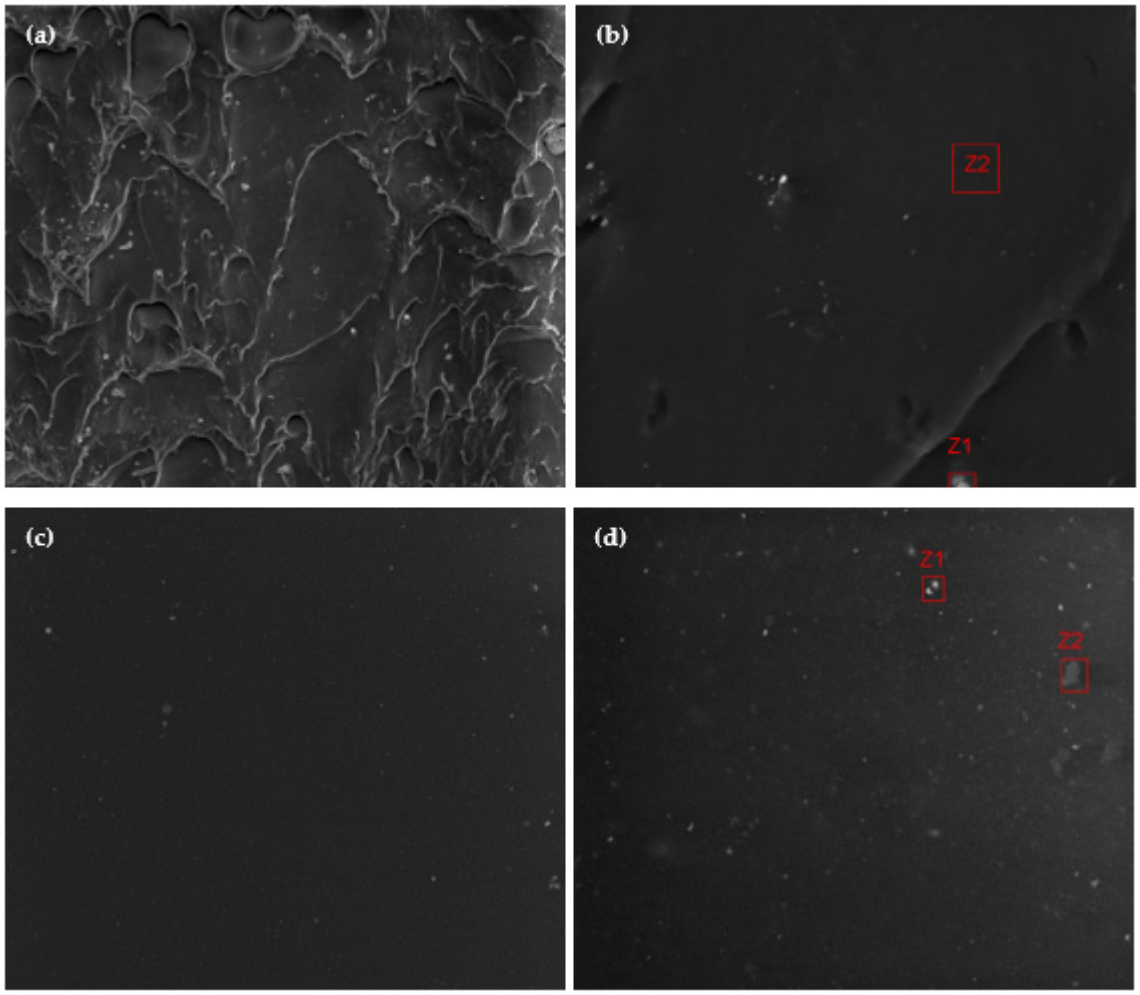


**Figure 6.** SEM images of: (**a**) polyurea A surface (magnification of 1000×), (**b**) highlighted zones on polyurea A surface (magnification of 5000×), (**c**) polyurea B surface (magnification of 1000×), (**d**) highlighted zones on polyurea B surface (magnification of 5000×).

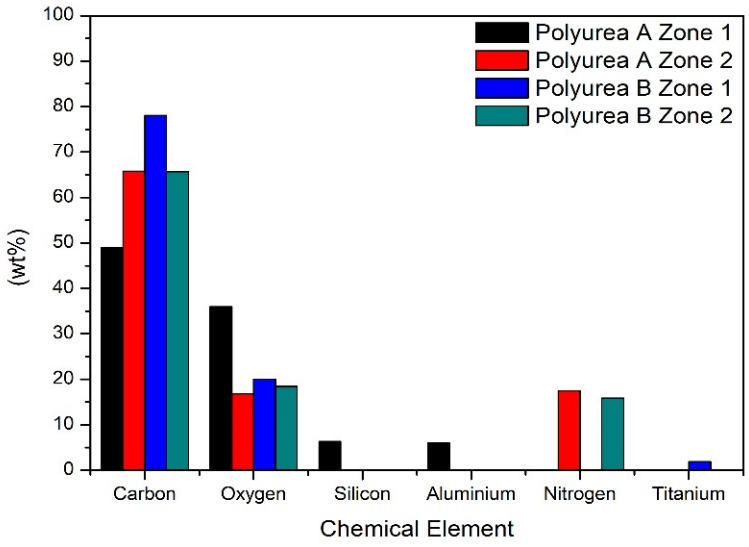


**Figure 7.** Comparison of the chemical composition of polyureas A and B obtained from the EDX technique.

**Table 1.** Density test results.

| Sample | Density ($g \cdot cm^{-3}$) |
|---|---|
| Polyurea A | $1.022 \pm 0.005$ |
| Polyurea B | $1.010 \pm 0.005$ |

The results from the dimensional stability test in Table 2 show that both polyureas used in this study present good dimensional stability since the dimensions in the longitudinal and transversal directions had minor variations.

**Table 2.** Dimensional stability test results.

| Sample | Longitudinal Direction Variation (%) | Transversal Direction Variation (%) |
|---|---|---|
| Polyurea A | 3.04 | 3.63 |
| Polyurea B | 4.25 | 5.38 |

### *3.4. Mechanical Characterization of the Polyurea*

The results for the Shore D hardness presented in Table 3 show polyurea A is harder than polyurea B. However, both samples have hard surfaces that can potentially withstand spall and reduce fragmentation against explosive blast.

**Table 3.** Shore D hardness test results.

| Sample | Duration of Test (s) | |
|---|---|---|
| | 3 | 15 |
| Polyurea A | $59 \pm 1$ | $57 \pm 1$ |
| Polyurea B | $44.4 \pm 0.8$ | $42.3 \pm 0.3$ |

The polyureas did not yield or rupture during the compression tests. Thus, the compression stress was determined at 10, 20, and 30% deformation (σ) for both polyureas. The results for the compression tests presented in Table 4 shows polyurea A has higher compressive strength than polyurea B in the deformation range of 10–20%. However, when the deformation increases to 30% the polyurea B presents higher compressive strength, which means it can withstand higher compression loads and deformations than polyurea A. The polyurea A has a higher compression modulus than polyurea B, despite the first presenting a microstructure that is less compact (it has a porous microstructure) than the latter.

**Table 4.** Compression test results.

| Sample | σ 10% (MPa) | σ 20% (MPa) | σ 30% (MPa) | Compression Modulus (MPa) |
|---|---|---|---|---|
| Polyurea A | $16.9 \pm 0.4$ | $21.3 \pm 0.5$ | $26.9 \pm 0.5$ | $314 \pm 0.0$ |
| Polyurea B | $8.4 \pm 1.8$ | $15.2 \pm 4.9$ | $37 \pm 21.4$ | $41.2 \pm 3.6$ |

The stress-elongation curves of both polyureas presented in Figure 8 are an example of the tensile behavior shown by these two polyureas. These stress-elongation curves can be divided into two distinct deformation regions, the elastic and the plastic. In the elastic region, the material has an elastic-like behavior. Thus, if the material does not reach its yield point, the deformation is fully recoverable if the load is off. On the other hand, if the material reaches its yield strength, it enters the plastic region, where the deformation becomes permanent and is not recoverable when the load is off. In case the load has not been removed, the stress reaches a maximum point, known as the tensile strength, and it breaks. The modulus of elasticity, known as Young's Modulus, which represents the

material's stiffness is calculated in the linear domain of the stress-elongation curve before the material reaches the yield stress.

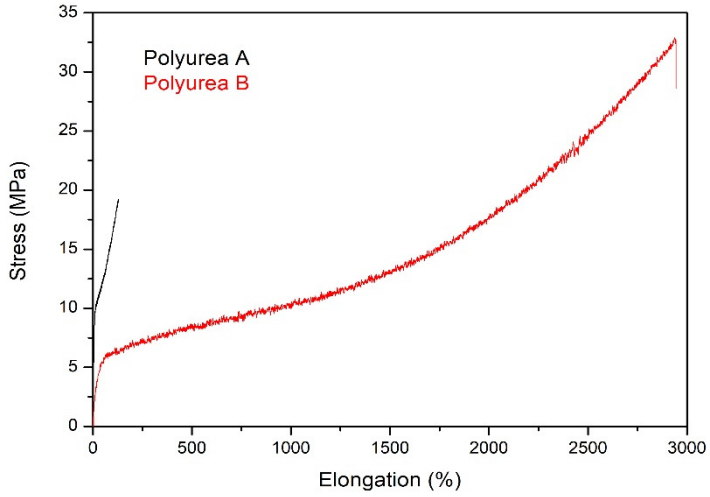


**Figure 8.** Comparison between the tensile properties of a specimen of polyureas A and B.

Table 5 summarizes the main properties obtained from the tensile tests performed on the polyurea. The tensile tests showed that polyurea B has exceptional mechanical properties, particularly the maximum elongation. This property is nearly 26 times higher in polyurea B than the maximum deformation presented by polyurea A. This remarkable ability to endure high deformations loads of polyurea B it is ideal to absorb the high frequency and intensity energy generated by explosion blasts.

**Table 5.** Tensile test results.

| Sample | Tensile Strength (MPa) | Maximum Elongation (%) | Young Modulus (GPa) |
|---|---|---|---|
| Polyurea A | 16.80 ± 1.84 | 113.61 ± 15.82 | 0.17 ± 0.03 |
| Polyurea B | 31.23 ± 2.04 | 2920.86 ± 43.98 | 0.03 ± 0.00 |

The excellent mechanical properties of polyureas are attributed to the physical crosslinking due to intermolecular and intra-molecular bidentate H-bonds between the urea linkages [13]. The polyurea exhibits a heterogeneous phase segregated microstructure, comprised of hard domains within soft domains [1,28]. The physical crosslinks (H-bonding), in the form of hard realms, that are dispersed throughout the polyurea matrix are responsible for the high elongation capability of this type of material. The excellent flexibility and elongation characteristics of the polyurea offer unique advantages for the structural enhancement of buildings. Since its nonlinear material behavior and dispersive wave propagation is ideal to contain spall and reduce fragmentation against explosive blast. The blast mitigation and ballistic protection characteristics of a polyurea are determined by its hard and soft domains, respectively [13]. The content of the hard segment of a polyurea in combination with the degree of phase separation (hard and soft phase) determines the mechanical properties of a polyurea system [29]. In the FTIR spectrum of both polyureas, presented in Figure 2, two peaks are present in the range of 1600–1700 $cm^{-1}$ attributed to the C=O stretching vibrations, with two nearby N-H in the urea group, which is conventionally called "ordered" bonding, that forms the hard phase (–NH–CO–NH–) of the polyurea. In addition to the chemical bonds present in both polyureas that contribute to the blast mitigation ability, the presence of titanium in polyurea B may have helped in the substantial increase of the tensile elongation of this material compared to polyurea A since titanium nanoparticles are commonly used in composites to improve the mechanical properties of materials.

As mentioned beforehand, the polyurea is an elastomer that, when subjected to blast and impact loads, tends to exhibit high strain to failure, thereby absorbing or dissipating the energy arising from dynamic loads. The characterization performed on both polyureas showed, especially the mechanical tests, demonstrated that polyurea B has more potential to be used as a coating in buildings for blast protection than polyurea A. Since this polyurea presents an exceptional capacity to absorb high deformations loads, which is a crucial characteristic to dissipate the energy generated during explosions and subsequent fragments.

## 4. Discussion

FTIR analysis of the two polyurethanes revealed similar spectra. The thermal characterization of the polyureas performed through DSC and TGA tests showed that both polyureas present two degradation stages. The first degradation stage that occurs around 300 °C, corresponds to a loss of mass attributed to the degradation of the hard segment part of the polyurea because of the relatively low thermal stability of the urea group. The second degradation stage, which starts around 400 °C is due to the decomposition of the soft segment. The two degradation stages of the polyurea resulted on a mass loss of 93.1%, and 96.3%, for polyureas A and B samples, respectively.

During the physical characterization of the polyureas, no significant differences were observed between the materials used in terms of density, water absorption, and dimensional stability. Observations of SEM tests displayed that the surface of polyurea A is heterogeneous while polyurea B has a more uniform and homogeneous surface. The EDX results show that both polyureas main elements are carbon, oxygen, and nitrogen. However, it should be mentioned that titanium was an element identified in polyurea B. Titanium is commonly used in composites to improve their mechanical properties. The Shore D hardness test results showed that both samples present a hard surface that can likely withstand spall and reduce fragmentation against explosive blast. The compression tests showed that polyurea A has a higher compressive strength than polyurea B, when the deformation is low, in the range of 10–20%. However, when the deformation increases to 30% polyurea B presents higher compressive strength which means it can withstand higher compression loads and deformations than polyurea A. Finally, the results from the tensile tests demonstrated that polyurea B has exceptional mechanical properties, especially in terms of maximum elongation, which is nearly 26 times higher than the maximum deformation presented by polyurea A. The high elongation behavior of polyurea B should provide excellent blast protection capacity. The presence of titanium in polyurea B may have helped the significant increase of the tensile elongation of this material compared to the polyurea A since titanium nanoparticles are commonly used in composites to improve the mechanical properties of materials.

## 5. Conclusions

In this study, using different characterization techniques, two commercially available polyureas were compared in terms of their physical, chemical, thermal, and mechanical properties, to evaluate their capacity to be used as used as protective coatings in buildings against blasts.

The characterization performed on the two polyureas showed that both materials presented comparable thermal properties, with similar degradation stages and temperatures. In the physical characterization of the polyureas, no relevant differences were realized between the two materials tested in terms of density, water absorption, and dimensional stability. Observations of SEM tests displayed that the surface of polyurea A is heterogonous while the other polyurea's surface is homogeneous. The chemical composition of both polyureas, ascertained using the EDX technique, is similar, with only the presence of titanium on polyurea B being the most relevant difference.

In conclusion, the mechanical characterization, the most important set of tests, performed on both polyureas determined that polyurea B has significantly better tensile properties-almost 3000% of maximum deformation capacity compared with approximately

115% of polyurea A, than the other polyurea. This exceptional capacity presented by polyurea B to endure high deformations loads makes for a drastic improvement compared with the tensile performance of polyurea A, which influences the choice of protective coating against blasts in the retrofitting of buildings.

**Author Contributions:** Conceptualization, C.M.; Investigation, F.L.; Project administration, C.M.; Resources, G.G. and J.M.; Supervision, J.B., F.C., R.F., G.G. and J.M.; Writing—original draft, F.L. All authors have read and agreed to the published version of the manuscript.

**Funding:** This research received no external funding.

**Institutional Review Board Statement:** Not applicable.

**Informed Consent Statement:** Not applicable.

**Data Availability Statement:** The data presented in this study are available on request from the corresponding author. The data are not publicly available due to privacy reasons.

**Conflicts of Interest:** The authors declare no conflict of interest.

## References

1. Choi, T.; Fragiadakis, D.; Roland, C.M.; Runt, J. Microstructure and Segmental Dynamics of Polyurea under Uniaxial Deformation. *Macromolecules* **2012**, *45*, 3581–3589. [CrossRef]
2. Mott, P.H.; Giller, C.B.; Fragiadakis, D.; Rosenberg, D.A.; Roland, C.M. Deformation of polyurea: Where does the energy go? *Polymer* **2016**, *105*, 227–233. [CrossRef]
3. Miao, Y.; Zhang, H.; He, H.; Deng, Q. Mechanical behaviors and equivalent configuration of a polyurea under wide strain rate range. *Compos. Struct.* **2019**, *222*, 110923. [CrossRef]
4. Szafran, J.; Matusiak, A. Polyurea coating systems: Definition, research, applications. *Parameters* **2016**, *2*, 103–110.
5. White, J.; Naskar, K. *Rubber Technologist's Handbook*; iSmithers Rapra Publishing: Shewsbury, UK, 2001; Volume 2.
6. Draganić, H.; Gazić, G.; Varevac, D. Experimental investigation of design and retrofit methods for blast load mitigation—A state-of-the-art review. *Eng. Struct.* **2019**, *190*, 189–209. [CrossRef]
7. Smith, P.D. Blast Walls for Structural Protection against High Explosive Threats: A Review. *Int. J. Prot. Struct.* **2010**, *1*, 67–84. [CrossRef]
8. Naito, C.; Dinan, R.; Bewick, B. Use of Precast Concrete Walls for Blast Protection of Steel Stud Construction. *J. Perform. Constr. Facil.* **2011**, *25*, 454–463. [CrossRef]
9. Knox, K.J.; Hammons, M.I.; Lewis, T.T.; Porter, J.R. *Polymer Materials for Structural Retrofit*; Air Force Research Laboratory: Eglin AFB, FL, USA, 1969.
10. Muszynski, L.C.; Purcell, M.R. Use of Composite Reinforcement to Strengthen Concrete and Air-Entrained Concrete Masonry Walls against Air Blast. *J. Compos. Constr.* **2003**, *7*, 98–108. [CrossRef]
11. Johnson, C.F. Concrete Masonry Wall Retrofit Systems for Blast Protection. Doctoral Dissertation, Texas A&M University, College Station, TX, USA, 2013.
12. Raman, S.N.; Ngo, T.D.; Mendis, P.; Pham, T. Elastomeric Polymers for Retrofitting of Reinforced Concrete Structures against the Explosive Effects of Blast. *Adv. Mater. Sci. Eng.* **2012**, *2012*, 754142. [CrossRef]
13. Iqbal, N.; Tripathi, M.; Parthasarathy, S.; Kumar, D.; Roy, P.K. Polyurea coatings for enhanced blast-mitigation: A review. *RSC Adv.* **2016**, *6*, 109706–109717. [CrossRef]
14. Wang, J.; Ren, H.; Wu, X.; Cai, C. Blast response of polymer-retrofitted masonry unit walls. *Comp. Part B Eng.* **2017**, *128*, 174–181.
15. Iqbal, N.; Sharma, P.K.; Kumar, D.; Roy, P.K. Protective polyurea coatings for enhanced blast survivability of concrete. *Constr. Build. Mater.* **2018**, *175*, 682–690.
16. Davidson, J.S.; Porter, J.R.; Dinan, R.J.; Hammons, M.I. Explosive Testing of Polymer Retrofit Masonry Walls. *J. Perform. Constr. Facil.* **2004**, *18*, 100–106.
17. Guo, H.; Guo, W.; Amirkhizi, A.V.; Zou, R.; Yuan, K. Experimental investigation and modeling of mechanical behaviors of polyurea over wide ranges of strain rates and temperatures. *Polym. Test.* **2016**, *53*, 234–244.
18. Baylot, J.T.; Bullock, B.; Slawson, T.R.; Woodson, S.C. Blast Response of Lightly Attached Concrete Masonry Unit Walls. *J. Struct. Eng.* **2005**, *131*, 1186–1193. [CrossRef]
19. Boubakri, A.; Guermazi, N.; Elleuch, K.; Ayedi, H.F. Study of UV-aging of thermoplastic polyurethane material. *Mater. Sci. Eng.* **2010**, *527*, 1649–1654.
20. Yılgör, E.; Yılgör, I.; Yurtsever, E. Hydrogen bonding and polyurethane morphology. I. Quantum mechanical calculations of hydrogen bond energies and vibrational spectroscopy of model compounds. *Polymer* **2002**, *43*, 6551–6559. [CrossRef]
21. Boubakri, A.; Elleuch, K.; Guermazi, N.; Ayedi, H.F. Investigations on hygrothermal aging of thermoplastic polyurethane material. *Mater. Des.* **2009**, *30*, 3958–3965.

22. Iqbal, N.; Kumar, D.; Roy, P.K. Emergence of time-dependent material properties in chain extended polyureas. *J. Appl. Polym. Sci.* **2018**, *135*, 46730.
23. Che, K.; Lyu, P.; Wan, F.; Ma, M. Investigations on Aging Behavior and Mechanism of Polyurea Coating in Marine Atmosphere. *Materials* **2019**, *12*, 3636. [CrossRef]
24. Arunkumar, T.; Ramachandran, S. Surface coating and characterisation of polyurea. *Int. J. Ambient. Energy* **2017**, *38*, 781–787. [CrossRef]
25. Awad, W.H.; Wilkie, C.A. Investigation of the thermal degradation of polyurea: The effect of ammonium polyphosphate and expandable graphite. *Polymer* **2010**, *51*, 2277–2285. [CrossRef]
26. Toutanji, H.A.; Choi, H.; Wong, D.; Gilbert, J.A.; Alldredge, D.J. Applying a polyurea coating to high-performance organic cementitious materials. *Constr. Build. Mater.* **2013**, *38*, 1170–1179. [CrossRef]
27. Delucchi, M.; Barbucci, A.; Cerisola, G. Crack-bridging ability and liquid water permeability of protective coatings for concrete. *Prog. Org. Coat.* **1998**, *33*, 76–82. [CrossRef]
28. Grujicic, M.; Pandurangan, B.; Bell, W.C.; Cheeseman, B.A.; Yen, C.F.; Randow, C.L. Molecular-level simulations of shock generation and propagation in polyurea. *Mater. Sci. Eng. A* **2011**, *10–11*, 3799–3808. [CrossRef]
29. Zhou, Q.; Cao, L.; Li, Q.; Yao, Y.; Ouyang, Z.; Su, Z.; Chen, X. Investigation of the Curing Process of Spray Polyurea Elastomer by FTIR, DSC, and DMA. *J. Appl. Polym. Sci.* **2012**, *125*, 3695–3701. [CrossRef]